Assessment of 3D Facial Scan Integration in 3D Digital Workflow Using Radiographic Markers and Iterative Closest Point Algorithm

Mohamed Elshewy
Marquette University

Assessment of 3D facial scan integration in 3D digital workflow using radiographic markers and Iterative Closest Point algorithm

by

Mohamed A. El-Shewy, BDS, MSc

A Thesis submitted to the Faculty of the Graduate School,

Marquette University,

In Partial Fulfilment of the Requirements for

the Degree of Master of Science

Milwaukee, Wisconsin

May 2020

ABSTRACT

ASSESSMENT OF 3D FACIAL SCAN INTEGRATION IN 3D DIGITAL WORKFLOW USING RADIOGRAPHIC MARKERS AND ITERATIVE CLOSEST POINT ALGORITHM.

Mohamed A El-Shewy, BDS, MSc

Marquette University, 2020

Introduction: Integration of 3 dimensional (3D) facial scanning into digital smile design workflows has been made available in multiple commercially available systems. Limited data exists on the accuracy of facial scans and accuracy of various methods of merging facial scans with cone beam computed tomography (CBCT) scans.

Objective: The purpose of this prospective clinical study was to evaluate the accuracy of 2 methods used to integrate soft tissue facial scans with CBCT scans. It would allow proposal of a novel approach for integrating a 3D facial scan using facial radio-opaque markers in a 3D digital workflow.

Material and methods: Fifteen CBCT and 3D face scans were obtained from patients who were undergoing treatment at MUSoD. A DICOM with RO markers and 3 STL data files from the facial scans were obtained for each patient. These files were superimposed using Exocad software. Accuracy of superimpositions was evaluated by measuring distances between RO markers on DICOM and STL data. The obtained dataset was analyzed using the paired t-test.

Results: The results showed that the mean values for the 6 subsets, merging through the ICP algorithm, were 1.47-2mm. However, when merged by RO markers, the mean value was 0.14mm. Using a paired t-test, the novel RO points method was statistically more accurate than ICP algorithm method (P<.001).

Conclusions: From the results of this study, it was concluded that the novel RO markers method offers improved clinical outcomes when merging 3D face scans with CBCT scans and can contribute to creation of a reliable digital virtual patient.

ACKNOWLEDGEMENTS

Mohamed A. El-Shewy, BDS, MSc

I would like to thank my God, for always being there with me and helping me accomplish this project.

I would like to express my deep and sincere gratitude to my mentor and advisor, Dr Geoffrey A. Thompson, director of the Graduate Prosthodontics program for his support generous effort, enormous support and supervision during this project research.

I would also like to thank Dr. Domagala Daniel for not only being a part of my committee but also for his enormous help and guidance.

I would like to express my deep thanks to Dr. Hongseok An for his great help, continuous guidance and support during this work

Special thanks to my family for believing in me and for their unconditional love and support throughout this work.

I would like to thank Marquette University and AAFP for sponsoring this project.

Lastly, I thank the patients who agreed to participate and make the study happen.

Without the guidance and help of these people this project would not have been possible.

TABLE OF CONTENTS

LIST OF TABLES

LIST OF FIGURES

LIST OF SYMBOLS AND TERMINOLOGY

Guide to Acronyms.

MUSoD	Marquette University School of Dentistry
2D	Two-Dimension
3D	Three-Dimension
CR	Centric Relation
VD	Vertical Dimension
VDR	Vertical Dimension at Rest
VDO	Vertical Dimension of Occlusion
HD	High Definition
DLM	Digital Laboratory Model
CAD/CAM	Computer Aided Design/ Computer Aided Manufacturing
CCD	Charged Couple Device
FOV	Field of View
CBCT	Cone Beam Computed Tomography
DICOM	Digital Imaging Communication in Medicine
STL	Standard Tessellation or Triangulation Language
OBJ	Object (format file)
AFT	Autofocus Tele (distance)
BB	Bite Block
DSD	Digital Smile Design
ICP	Iterative Closest Point

MeSH	Medical Subject Headings
PLY	Polygon (standard triangle)
SPG	Stereophotogrammetry
PG	Photogrammetry
LB	Laser Beam
SLS	Structured Light Scanning
VPM	Vertical Patient Model
NHP	Natural Head Position
DSLR	Digital Single Lens Reflex
IOS	International Organization Standardization
OEMs	Original Equipment Manufacturers
NoseAlg	Nose Algorithm
NoseMark	Nose Markers
RChAlg	Right Cheek Algorithm
RChMark	Right Cheek Markers
LChAlg	Left Cheek Algorithm
LChMark	Left Cheek Markers
RErAlg	Right Ear Algorithm
RErMark	Right Ear Markers
LErAlg	Left Ear Algorithm
LErMark	Left Ear Markers
MentAlg	Mental Algorithm
MentMark	Mental Markers

Explanation of Digital Dental Terms

General Term	Explanation or definition
3D data files format for creating and storing	For example: ply, obj and STL. The STL file format is commonly used for many open platforms dental scanning and design systems.
3D modelling	Process of developing a digital representation of any 3D object surface via specialized software.
3D rendering	Computer graphics process of automatically converting 3D wire frame models into 2D images with 3D photorealistic effects on a computer.
3D printing	Additive manufacturing processes that build 3D structures by depositing layers of material on top of each other until the final structure is achieved.
3D scanner	A device that analyzes a real-world object to collect data on its shape or color or texture.
3D surface scanning	Surface mapping that allows for the surface geometry or shape of an object to be stored as a set of 3D points or vertices or as a series of polygons (or faces).
CAD/CAM dentistry	Computer-aided design and computer-aided manufacturing Using computer technologies to design and produce different types of dental restorations.
Computer-Aided Design (CAD)	The use of computer programs to create (2D or 3D) graphical representations of physical objects.

Digital Imaging and Communications in Medicine (DICOM)	Standard for handling, storing, printing, and transmitting information in medical imaging. Including file format.
Cone Beam Computed Tomography (CBCT)	A medical imaging technique using a cone beam of X-ray computed tomography where It allows for the collection, storage, and utilization of 3D radiographic data in the DICOM file format,
Image stitching	The process of combining multiple photographic images with overlapping fields of view to produce a segmented panorama or high-resolution image
Intraoral scanning	The process of scanning and capturing the intraoral cavity for translation into a digital file format, such as STL.
Milling	The machining process of using rotary cutters (burs) to remove material from a workpiece to fabricate dental restorations with high precision.
Model scanning	The process of acquiring the 3D image of a dental model for translation into a digital file format, such as STL and used in a CAD software program for the design and fabrication of a dental prosthesis.
OBJ	Simple data-format file that represents 3D geometry alone: the position of each vertex, position of each texture coordinate vertex, normal, and the faces that make each polygon defined as a list of vertices and texture,

Optical scanners	Devices that use light projection or laser beams to obtain a 3D digital replica of an object.
Photogrammetry	The practice of determining the geometric properties of objects from photographic images.
Standard tessellation language (STL)	File format native to the stereolithography CAD software created by 3D Systems. This file format is supported by many other software packages, STL file describes only the surface geometry of 3D object without any representation of color or texture.
Stereophotogrammetry	A method used to estimate the 3D coordinates of points on an object. These are determined by measurements made in two or more photographic images taken from different positions by camera.
Structured-light 3D scanner	Scanning device used for measuring 3D shape of an object using projected light patterns and a camera system.
Tessellation	The division of a surface into smaller polygons, yielding a higher level of detail.

CHAPTER I
INTRODUCTION

Diagnosis and treatment planning are essential elements for successful oral rehabilitation.[1] Integration of 3D facial scanning into digital smile design workflows has been made available in multiple commercially available systems. Limited data exists on the accuracy of facial scans and accuracy of various methods of merging facial scans with CBCT scans. The use of anatomic landmarks on the patients' face is helpful when determining size and position of teeth during digital waxing in the diagnostic part of prosthetic rehabilitation.[2] 3D face scans can be used to visualize treatment outcomes and enhance doctor-patient and doctor-technician communication.[3]

In prosthetic rehabilitation, the dentist must meet the functional and esthetic demands of the patient. Smile design should be guided by and integrated with the patient's facial references such as facial midline, lip line and smile line. Information related to the patient's skeletal, dental, as well as, soft tissue profiles can be used for diagnostic evaluation.[4,5] Conventional prosthodontic evaluation is based on study casts, photographs and radiographs. Because of the 2D nature of photographs and radiographs, information transfer to 3D model is difficult and may result in error.[6]

The introduction of dental 3D facial scanning revolutionized the principle of virtual designing and fabrication of a digitally based prosthetic appliance through a reconstructed 3D virtual image.[7,8]

CHAPTER II
LITERATURE REVIEW

1-Facial scanners:

Enhanced predictability of treatment planning may be achieved by incorporating 3D face scans with dental design software.[9] 2D photographs may be helpful during dental treatment planning but may present significant limitations when used to accurately reconstruct a 3D object.

3D scanning devices used for the head and neck can be classified into 2 groups: 1) Internal – scanners able to capture soft and hard tissues, and 2) External – surface scanners. Internal scanning devices use a high dose of radiation to produce an image. Patient exposure to radiation, image distortion related to metal and the high cost of equipment ownership are reasons why internal scanners have not gained popularity as compared with surface face scanners.[10,11]

External scanners gained popularity among clinicians in recent years. The different types of technologies used in external scanners can be classified as follows: Dual structured light with infra-red sensor (DSLS); structured light scanning (SLS); Photogrammetry (PG); laser beam scanning (LB); and stereophotogrammetry (SPG).[12] Advantages and disadvantages of each technique can be summarized in Table1i.[13] When compared with internal scanners, external scanners have lower cost, are minimally invasive and rapid.[14,15]

	LB	SPG	PG	SLS	DSLS
Invasive	Non	Non	Non	Non	Non
Accurate	Yes	Yes	Yes	Yes	Yes
Number of scans	Various	One scan	Various	Various	one scan
Reproducible	Yes	Yes	Yes	Yes	Yes
Eye safety	Yes	Non	Non	Non	Non
Calibration	Yes	Yes	Yes	Yes	Auto
Sensitivity to light	Yes	Yes	Yes	Yes	Yes

Table 1i. Advantages and disadvantages of technologies used in facial scanning.

SLS 3D scanning systems are devices using a precise method of structured light based on phase measuring profilometry, where the system consists of a charged coupled device (CDD) camera, 3 mirrors and a projector. After projecting the grating on the face, the resultant deformation records the right, then the left faces, and consequently, through 2D images by the camera.[16,17]

The laser scanning system is a low cost, accurate 3D imaging system that gained popularity for its ease of application in craniofacial and soft tissue imaging. It is used to evaluate changes in facial morphology associated with either growth or non-surgical treatment.[18]

Stereophotogrammetry is a rapidly evolving 3D facial technology that has already been used by many industries. It uses a digital archive process which requires the acquisition of high-quality images. Good control of the image capture process may be considered a challenge to new users.[19] It has been introduced to dentistry in 3D digital workflows to obtain a complete virtual patient model (VPM) and to record a Natural Head Position (NHP) for the patient.[20,21] This technology scans and records the patient's external profile and it can be used in any dental office using a small compact and inexpensive scanner. The scanner is user friendly because image acquisition can be done within seconds. Scans can be merged in any available Computer-Aided Design/Computer-Aided Manufacturing (CAD/CAM) digital workflow systems.[22]

Other methods for scanning facial soft tissues are direct (2D) photogrammetry, anthropometry, CBCT and lateral cephalometry.[23,24,25,26] CBCT uses ionizing radiation.[27] 2D photogrammetry and lateral cephalometric methods, produce facial soft tissue images with distortion, magnification and inaccuracy in facial measurement.[28] In 2010 Kochel et al. concluded that the limitations of 2D can be overcome by using 3D SPG with acquisition of facial scans with high color resolution in a short time which can integrated with digital software according to the clinical purpose.[29] In 2016 Dindaroğlu et al. reported that 3D SPG provides accurate images for facial soft tissues.[30]

Digital workflows in CAD/CAM have been introduced to dentistry to automate design and manufacturing processes of simple and complex restorations.[31,32] Intraoral scanners, CBCT, extra-oral scanners are devices used for acquisition of data used in diagnosing, treatment planning and later in fabrication of prostheses.[33]

One of the most valuable techniques for convincing a patient to move forward with the proposed treatment is what has been traditionally termed a “mock-up’ or trial smile or esthetic prototype which can better demonstrate what is being planned.[34,35]

2-Digital Smile Design (DSD):

Digital Smile Design (DSD) is a technical novelty whereby the patient’s smile is pre-visualized and simulated allowing the dentist to plan the treatment. This allows the patient to reach consensus with the dentist regarding the expected outcome.[36]

Advances in digital imaging and programs specifically designed for a dental application like DSD make it possible to show patients a preview of their digitally enhanced and manufactured smile. It can be both a communication and motivational tool used by dentists and technologists before attempting any treatment.[37] In 2015 Zimmermann and Mehl reported that the smile design process depends upon photography, image alignment and definition of reference lines, calibration, 2D smile frame definition, lip line, smile curve tooth shape, facial morphology (texture, color) and transformation of 2D into 3D design.[38]

In 2012 Coachman and Calamita developed a concept of DSD technique for orofacial rehabilitation. This technique integrates photography with digital CAD producing enhanced smile visualizations that look very realistic.[39] Coachman et al.2017, integrated 3D facial scans into his digital workflow instead of 2D photographs. 3D DSD was introduced as a tool for communication with patients who have specific esthetic demands.[40]

3-Digital 3D Stereophotogrammetry (SGP):

Facial appearance cannot be realistically reproduced with good results using 2D computer graphics.[41] Since the 1980's, the focus has been on the 3rd dimension, as a way to overcome deficiencies of 2D imaging and stereophotogrammetry.[42]

Moro et al. 2009, reported that the merging of 3D digital imaging techniques is a reliable and accurate for facial analysis.[43]

In 2010 Heike et al. reported that the 3D digital SPG is the most popular 3D soft tissue imaging technology. The observation was made that it is a robust tool that may be used to scan craniofacial structures. SPG possesses distinct advantages to include: minimal invasiveness, high accuracy and rapid capture of the faces shape and texture. It was reported that 3D digital Stereophotogrammetry is becoming the most well-liked facial surface imaging modality and it performs well when integrated with CBCT scan.[19]

Naudi et al. in 2013 studied the effect of concurrent capture of the 3D surface of the face by stereophotogrammetry and CBCT scan of the skull on the accuracy of registration and superimposition. They concluded that the concurrent capture of digital 3D surface scanning and CBCT scan significantly enhances the accuracy of registration and superimposition of these imaging methods.[44]

Development of 3D imaging led to a wide implementation of this technology within the dental profession and its different specialties. Reproduction of a virtual 3D facial appearance model or replica entails fusion of information obtained from digital radiographic scanners and surface scanning.[45,46]

Wavefront Technologies developed extra-oral 3D facial scanning where exported data is saved in the geometry definition format "object file" (OBJ). This allows storage of the 3D shape information, surface texture, and shading with surface color. The STL file format contains information about triangulated surface geometries of 3D digitized object but it is lacking color and texture information.[13,47]

Multiple publications studied the repeatability and accuracy of merging extra oral and intraoral scanning with CBCT. It has been well-documented that merging surface scans with CBCT is clinically acceptable.[6,13,20,48,49] Leon et al. in 2019 described the digital workflow procedure for designing lithium disilicate laminate veneers using intraoral scanning, computed tomography and CAD/CAM software. The merged data from a digital diagnostic waxing and the patient's photographs was exported and used as a reference for restoration design and fabrication.[3,50] CAD/CAM technology has been an integral part of the clinical and laboratory steps in restorative dentistry.[51]

4-Exocad software:

Exocad software has been chosen by leading OEMs worldwide for integration into their dental CAD/CAM offerings. It is a powerful dental software for integrative workflow for scanners, mills, printers and cameras to work together. This software is fast, easy to handle and it can create esthetic and functional restoration designs. Exocad offers a flexible workflow, and it can deliver a same-day-restoration in the dental practice and facilitate communication with dental laboratories for improved and predictable outcomes. It can integrate open platform hardware with the material of choice and it is easy to learn the step-by-step process.[52]

5-CBCT:

CBCT is 3D volumetric imaging advanced modality which has many advantages including provision of high diagnostic quality images with sub-Millimeter resolution, short scan time of about 10-70 second and lower exposure dose of radiation. A major advantage of CBCT is that the entire maxillofacial region can be imaged through a single scan and with minimal distortion.[53]

6-CBCT Principle:

The CBCT scanner is based on the principle that consists of the source of a cone shaped X ray beam, the flat panel detector which captures serial slices, all mounted on a rotating gantry which rotates once around the patient. Captured data is reconstructed by computer algorithm to provide sequential series of cross sectional images and 3D volumetric rendering.[54] DICOM format (Digital Imaging and Communications in Medicine) is used to export from CBCT to allow ease of telecommunication and merging with other digital imaging software. Dental software program can be used to view and manipulate DICOM files.[55]

7-Merging digital workflows:

Lee et al. in 2012, described a technique of fusing a DICOM file with an STL files acquired from an intraoral scanner. Both files were electronically sent to a 3D imaging software company to produce a graphic model of the jaws and surgical template for surgical implants.[56]

In 2008, Maal et al. concluded that the 3D merging of the DICOM file and 3D facial stereophotogrammetric scanning results in an accurate and realistic 3D digital facial presentation of the patient. It was concluded that dental surgeons could use this data set as a diagnostic method for treatment planning, postoperative evaluation and for patient communication.[57]

In 2019 Cascon et al. reported on the rehabilitation of an edentulous maxilla guided by facial landmarks and CAD/CAM technology. A digital workflow using extra-oral scanning and CBCT imaging was utilized to obtain a 3D virtual registration of the patient's face. It was concluded that the novel digital workflow in which the baseplate and occlusion rims which were designed in open-source software, can produce successful treatment outcomes and reduce laboratory cost and time.[58]

In 2008 Rangel et al. described integration of facial scanning with digitized dental casts. Their study was conducted on healthy orthodontic patients with normal dentition. While employing a special Iterated Closest Point algorithm (ICP) software, they integrated a digital dental cast with a digital 3D image of the patient in the closed and open positions. Collected data sets were matched and resulted in a visible dental cast through a semi-transparent facial picture.[6]

In 2015 Joda et al. concluded that fusion of the various data file formats (STL, OBJ and DICOM) can be adjusted through common reference points.[20] Hassan et al. 2016 advocated that integrating facial scans with digital models is an important part of planning when rehabilitating edentulous patients with an implant supported prosthesis (Digital try-in stage).[49]

8-Extra-oral facial scanning using a smart mobile phone:

Daher et al. in 2018, suggested that a smart phone could be used as a simple and accessible tool for entering a digital workflow as it can be used as a 3D extra-oral facial scanner. This development is favourable for many dentists who might not have access to digital impression devices and procedures. They concluded that the 3D workflow increases the realism of digital smile simulations. It allows for presentation of the proposed treatment outcomes from multiple view angles and printing of the virtually designed models in 3D. It also allows for making silicone keys, printing in polychromatic esthetic composite or milling of ceramic restorations.[59]

9-Facial scanning using Bellus3D technology:

Photogrammetry is the science and technology of obtaining reliable information about physical objects and the environment through the process of recording, measuring and interpreting photographic images and patterns of electromagnetic radiant imagery and other phenomena. The process can include 3D scan features such as color and texture. The Bellus3D Apple iPhone X application is a remarkable advancement in face scanning technology.

The 3D facial scanning application is able to capture a facial scan with 250,000 data points using a smartphone in an average 10 seconds while the patient is turning their head. The face is then virtually reconstructed in 3D with high details. The resulting image can be zoomed and rotated in 3D on the iPhone screen. The Bellus3D App is very fast, precise and includes interactive review of the 3D face scan. The files can be stored and aligned with the PLY, STL, CBCT scans and other intraoral files stored in the patient's digital planning folder.[60]

Alignment Face Teeth (AFT) dental system consists of the Bellus3D camera attached to a cell phone (Apple iPhone X or iPad). It is a fast and precise 3D face scanning system (<15 seconds). The system uses bite blocks which allow merging of diagnostic casts (3D models) with the facial scan.[61]

Classical prosthodontic evaluation is based on study casts, photographs and radiographs which are typically a 2D representation of the patient and use of 3D facial scans merged with other digital data files is limited. Therefore, the null hypothesis was that there would be no difference between the merging CBCT and 3D facial scanning using an ICP algorithm and a novel approach.

CHAPTER III
MATERIALS AND METHODS

Study protocol:

Approval for this prospective clinical study was requested and obtained from the Marquette University School of Dentistry (MUSoD) Institutional Review Board, HR-1901027582.

Using the 2-sided paired t test and a significance level of .05, a sample size of 15 was found to be sufficient with a power of .80.

Fifteen individuals requiring a CBCT for treatment planning and prior to clinical restorative care were recruited from among patient's seeking care at MUSoD. All patients agreed to participate in the clinical study and were informed about the purpose of the study and associated procedures. Each patient was given informed consent, allowed time for questions and then signed the consent form. In addition, a photogrammetric analysis was made for the purpose of acquiring a 3D image of each participant's face in repose and at smile.

Materials needed for digital workflow:

- RO markers were used for orientation of facial planes for 3D Digital Smile Design (DSD).

- Alignment Face Teeth system (AFT System One) consists of Bellus3D camera attached to a tablet and it was used for the facial scanning. AFT is a simple and fast system that allows obtaining all the necessary information of the patient's face in 3D. Facial scanning can be saved digitally as an Object (OBJ) file which is a geometry definition file format. The file format is open and has been adopted for 3D objects.

- Forehead Aligner Band (FAB) was used to integrate the smile facial scan with the repose facial scan.

- Bite block (BB) was made using autopolymerizing bite registration material (Futar D-fast, Kettenbach) and it was used for recording the occlusal relationship. Futar D bite registration material is a syringeable elastomer with high final hardness.

- CBCT scan was acquired using Planmeca 3D machine (Sordex Scanora, Finland) and exported as a DICOM file.

- Exocad software was used for merging files (STL, OBJ and DICOM) by Iterative Closest Point (ICP) algorithm software. ICP is a surface matching algorithm applied to bring 3D surface facial scans into maximum alignment.

Methods (Workflow procedures):

The AFT system was used to capture a 3D picture of each individual. The AFT includes a Bellus 3D camera (Fig. 1) which is a 3-lens camera that is connected to a tablet, a forehead aligner band (Fig. 2), tablet mount and a tablet with Bellus 3D software.

Figure 1. Bellus3D Camera.

Figure 2. Forehead Aligner Band.

Calibration of the camera facial scanner (AFT):

Calibration was made for standardization of the facial scanning procedure between each patient. Calibration included 3 parameters: 1) the distance from the scanner to patient's face; 2) height of the 3D camera and 3) the angle of the 3D camera.

Thirty millimeter horizontal and vertical lines originating from the same point were made at right angles to each other and drawn over a manikin's forehead. Different facial scans were taken at different distances, angles and heights until the measurements of the 2 lines and the angle on the facial scan were closest to reality.

The tablet was placed at 76.2 cm height, and 50.8 cm distance from the patients' face and at a 60-degree angle (Fig. 3). The Bellus3D software has a face area on the capture screen which turns green if the patient's head position is at the correct distance and angle (Fig. 4).

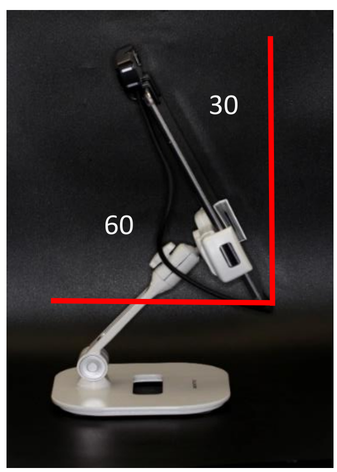

Figure 3. The tablet placed at 76.2 cm height, 50.8 cm distance from the patient's face at a 60-degree angle.

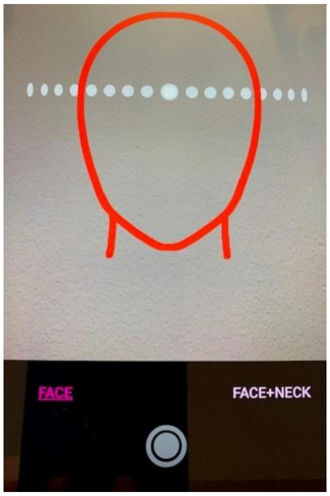

Figure 4. Bellus3D has a face area on the capture screen.

The workflow used for digital merging:

A-RO markers

B-Forehead aligner band

C-Bite block

D-CBCT

E-Facial scan

F-File merging

A-RO markers insertion:

Figure 5. Suremark Labels RO markers.

At the CBCT appointment, 6 RO markers (Fig. 5) were placed onto the patient's face in the following positions: 1) 1 RO marker on the tip of the nose and in the facial midline (Nose); 2) 2 RO markers on the lowest points of the orbital rim (Right Cheek: RCh and Left Cheek: LCh); 3) 2 RO markers at arbitrary hinge axis location (Beyron's point); (Right Ear: REr and Left Ear: LEr); and 4) 1 RO marker in the middle of the mental region in the facial midline (Ment). These RO markers allow integration of the repose and smiling facial photogrammetric scans with the CBCT imaging scan (Fig. 6).

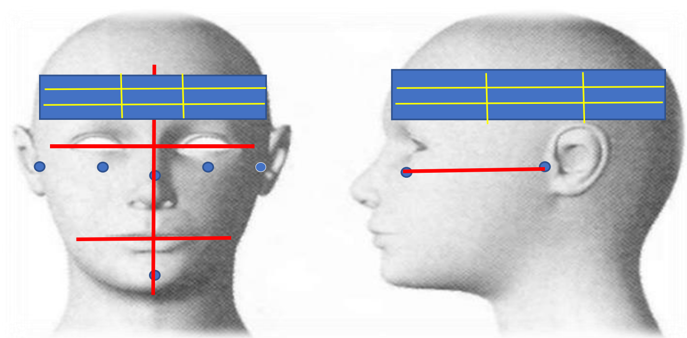

Figure 6. Forehead aligner band and radio-opaque (RO) markers placed at 6 facial locations.

B-Forehead aligner band:

Each patient was asked to wear a forehead aligner band (Figs. 6 and 7). This band was used to integrate the facial scan at smile with a facial scan in repose.

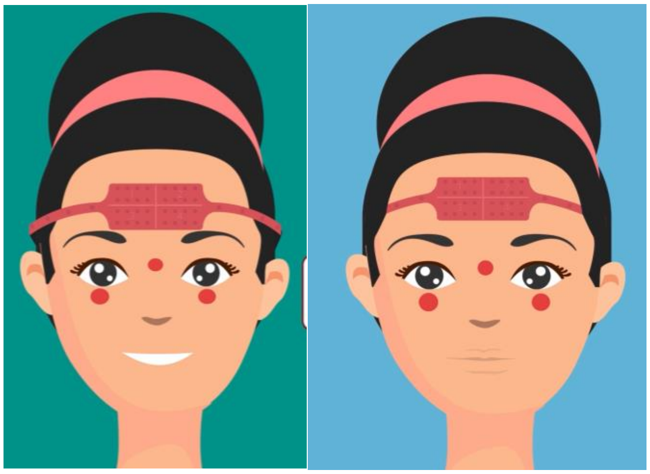

Figure 7. Forehead aligner band for smile and repose facial photogrammetric scans. (Figure is used with permission by AFT).

C-Bite block (BB):

Futar D-fast bite registration material (Fig. 8) was used to make a BB for each patient. A jaw relation record was made in centric relation (CR) at a proposed vertical dimension (VD) in cases that require restoration of vertical dimension. The patient was asked to swallow and pronounce “Emma” a few times until vertical dimension at rest (VDR) was observed, then the bite registration material was extruded over the teeth and the patient is asked to close approximately 2mm from VDR. In other instances where the VD was acceptable, the patient was asked to close into CR while using a bimanual manipulation method. The BB was trimmed and rechecked.

Figure 8. Futar D-fast bite registration material for making bite block (BB).

D-CBCT acquisition:

CBCT scans were acquired using a 3D X Planmeca (Sordex Scanora, Finland) with a field of view of 14 cm (W) × 16.5 cm (H). The technical specifications of the CBCT unit according to the manufacturer are: 90 kVp, 10 mAs and 2.4 sec. Images were acquired in standard resolution with a voxel size of 0.3mm, dose radiation DAP-1526 (mGy.cm2) and effective dose of 234 micro Sieverts (μSv).

Each patient was seated and adjusted in the chair for CBCT acquisition with the RO markers in place. The BB was then inserted, and the patient was asked to close their mouth. CBCT scans were acquired and exported in a DICOM data file format (Fig. 9).

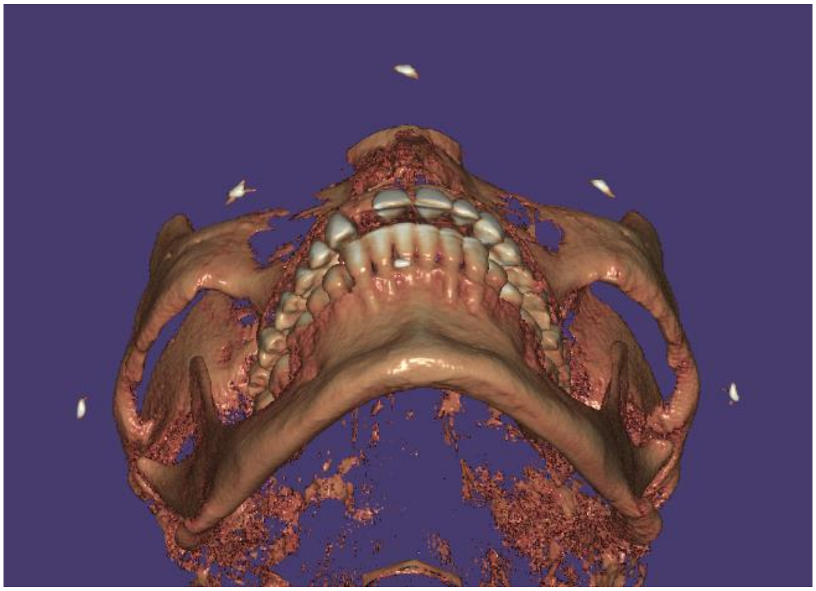

Figure 9. CBCT 3D volumetric rendering scan with visible RO markers.

E-Facial scan AFT:

The first facial scan was taken under the same conditions as the CBCT and with the patient biting on the BB. The Bellus3D camera was connected to the tablet and mounted on the stand, it was then placed in front of the patient at the standardized and calibrated distance, angle and height. The patient was asked to look at the camera and rotate their head to the right and then the left while keeping their head in the center of the face area on the iPhone. The facial scan file was saved and exported as an OBJ file (OBJ-Repose). The second facial scan was taken after removing the BB and the patient was asked to smile (OBJ-Smile) while they were wearing the forehead aligner band (Fig. 10).

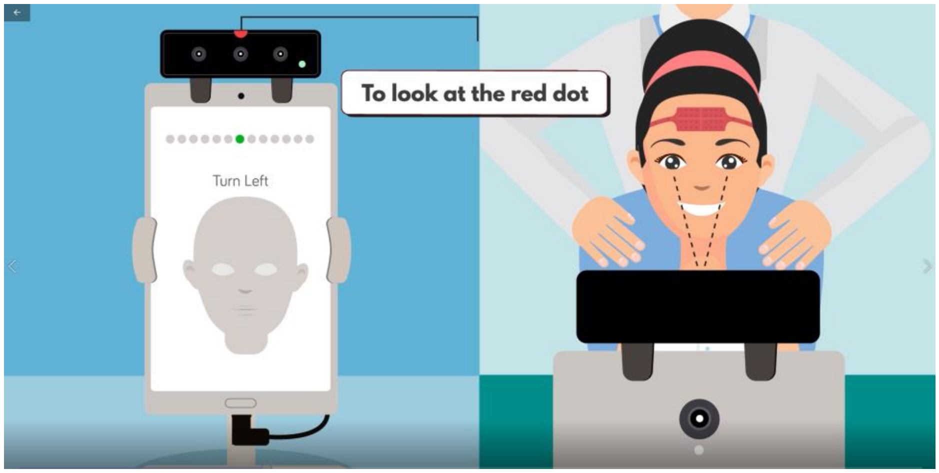

Figure 10. Facial scan by AFT using Bellus3D Camera.

(Figure used with permission by AFT).

F-File Merging:

The CBCT DICOM file, 2 facial scans (OBJ-Repose and OBJ-Smile) were uploaded and opened in the Exocad software. The OBJ-Repose file obtained from the facial scanner was merged with the CBCT DICOM file using 2 different techniques:

1) ICP algorithm: The OBJ-Repose file was approximated to the soft tissue profile of the CBCT by manual movement. Then, pressing on "best fit match" option to fine tune the alignment by ICP algorithm (Fig. 11), and

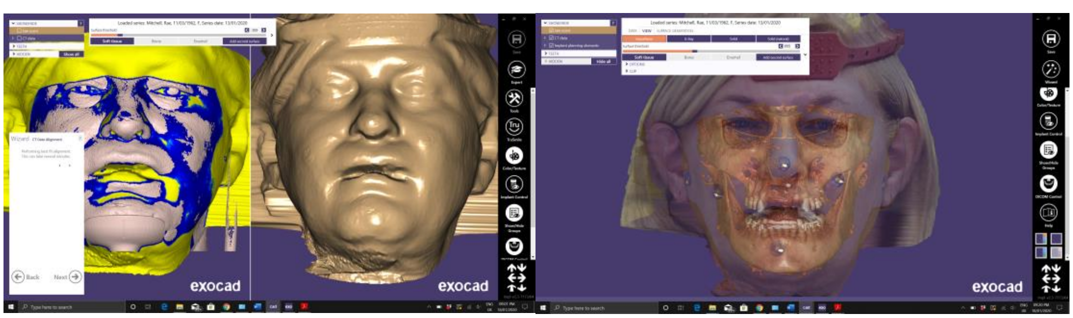

Figure 11. ICP algorithm software.

2) Radio-opaque (RO) markers: The second method was performed manually using the option "Align Meshes". This was accomplished by selecting RO markers on the floating

mesh (facial scan: OBJ-Repose) and matching them with their corresponding radiographic markers on the fixed mesh (CBCT) and then performing a manual alignment by matching of markers (Fig. 12).

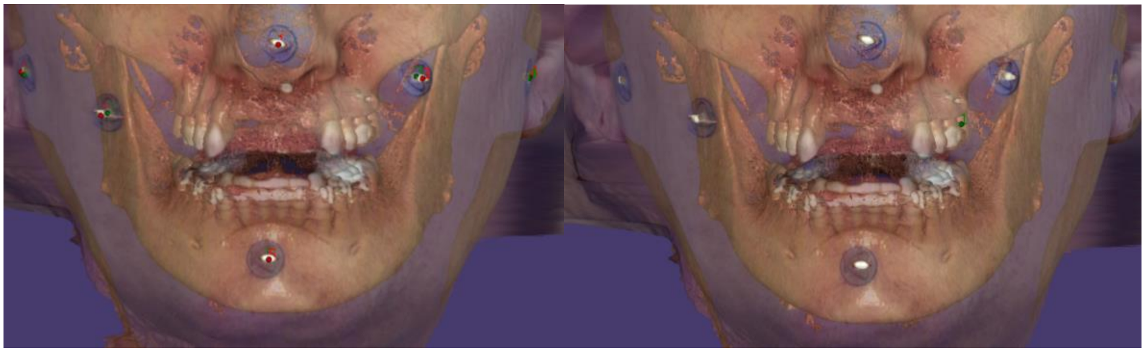

Figure 12. Alignment of meshes using RO markers.

The forehead aligner band was not used to align the OBJ-Smile to OBJ-Repose which was already merged with the CBCT. This technique allows for merging of the smile facial scan with the CBCT (Fig. 13).

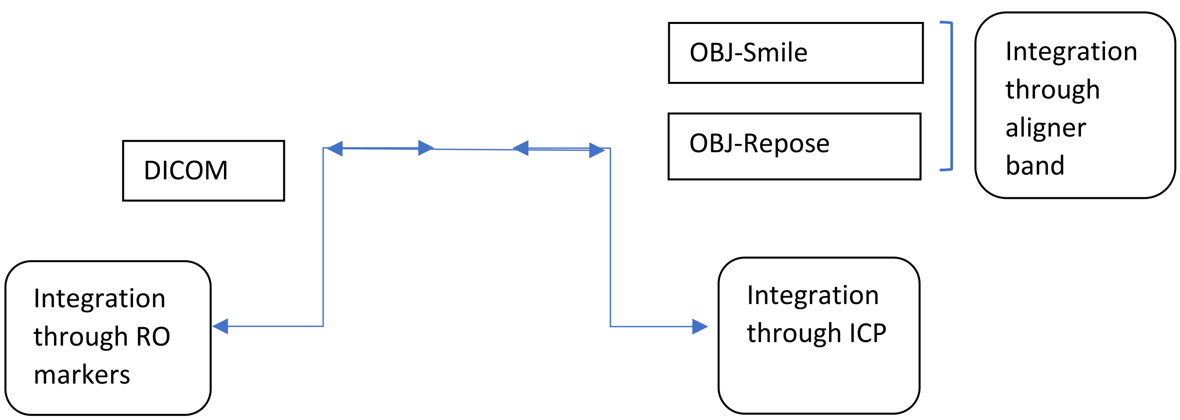

Figure 13. Schematic diagram of integration for different digital workflows.

Measurement of the accuracy of the merging:

The distances between the RO point markers on the facial scans and the corresponding markers on the CBCT were measured at each point to evaluate accuracy of the ICP algorithm method. Means and standard deviations at each point were determined. Two tables were created for the 6 points and for each of the 15 patients, one for each technique (Fig. 14).

Figure 14. Showing Accuracy measurement of the Iterative Closest point algorithm method.

A Paired t-test was used to compare accuracy of ICP algorithm method and RO point marker method at each point. The statistical analysis was conducted using statistical software (IBM® SPSS® Statistics version 26). The null hypothesis assumed that the paired population means were equal, where the alternative hypothesis assumes that the paired population means were not equal.

H0: $\mu 1 = \mu 2$

H1: $\mu 1 \neq \mu 2$

CHAPTER IV
RESULTS

The results were divided into 2 main groups. The first group, n=15, merging through ICP algorithm was divided into 6 subsets representing points marked: Nose, RCh and LCh, REr and LEr and Ment. The second group, n=15, merged through RO markers was divided into 6 subsets representing points marked: Nose, RCh and LCh, REr and LEr and Ment.

The results of the 6 Paired t-tests conducted for each of the 6 paired subsets were summarized in 3 tables as follow: Paired Samples Statistics, Paired Samples Correlations, and Paired Samples Test, followed by analysis for each one.

First pair of Subsets Nose:

Paired Samples Statistics

		Mean	N	Std. Deviation	Std. Error Mean
Pair 1	NoseAlg	1.47	15	.93	.24
	NoseMark	.14	15	.15	.04

Table 1.1. First pair of subsets Nose-paired samples statistics.

Paired Samples Correlations

		N	Correlation	Sig.
Pair 1	NoseAlg & NoseMark	15	.038	.89

Table 1.2. First pair of subsets Nose-paired samples correlation.

Paired Samples Test

		Paired Differences					t	df	Sig. (2-tailed)
		Mean	Std. Deviation	Std. Error Mean	95% Confidence Interval of the Difference				
					Lower	Upper			
Pair 1	NoseAlg - NoseMark	1.32	.94	.24	.80	1.84	5.430	14	.000

Table 1.3. First pair of subsets Nose-paired samples test.

Tables 1.1-1.3 show the descriptive statistics of the first pair of subsets Nose, where the mean and standard deviation of the NoseAlgorithm subset were 1.47 and 0.93 respectively, while the mean and standard deviation of the NoseMark subset were lower 0.15 and 0.04 respectively, which means that the average of measuring differences was lower in the merging through markers than algorithm. NoseAlgorithm and NoseMark subsets were weakly and positively correlated ($r=.038$, $P>.001$). Finally, there was a significant difference between NoseAlgorithm and NoseMark subsets ($t_{14}=5.4$, $P<.001$), which means that merging by markers was significantly more accurate than merging by algorithm.

<u>Second pair of Subsets RCh:</u>

Paired Samples Statistics

		Mean	N	Std. Deviation	Std. Error Mean
Pair 2	RChAlg	2.00	15	1.62	.42
	RChMark	.13	15	.16	.04

Table 2.1. Second pair of subsets Right Cheek- paired samples statistics.

Paired Samples Correlations

		N	Correlation	Sig.
Pair 2	RChAlg & RChMark	15	-.021	.079

Table 2.2. Second pair of subsets Right Cheek- paired samples correlation.

Paired Samples Test

		Paired Differences					t	df	Sig. (2-tailed)
		Mean	Std. Deviation	Std. Error Mean	95% Confidence Interval of the Difference Lower	95% Confidence Interval of the Difference Upper			
Pair 2	RChAlg - RChMark	1.87	1.66	.43	.95	2.79	4.352	14	.001

Table 2.3. Second pair of subsets Right Cheek- paired samples test.

Tables 2.1-2.3 show the descriptive statistics of the second pair of subsets Right Cheek, where the mean and standard deviation of the RChAlg subset were 2 and 1.6 respectively, while the mean and standard deviation of the RChMark subset were lower 0.13 and 0.04 respectively, which means that the average of measuring differences was lower in the merging through markers than algorithm. RChAlg and RChMark subsets were weakly and negatively correlated (r=-0.2, P>.001). Finally, there was a significant difference between RChAlg and RChMark subsets (t_{14}=4.3, P<.001), which means that merging by markers was significantly more accurate than merging by algorithm.

Third pair of subsets LCh:

Paired Samples Statistics

		Mean	N	Std. Deviation	Std. Error Mean
Pair 3	LChAlg	2.09	15	1.47	.38
	LChMark	.13	15	.15	.04

Table 3.1. Third pair of subsets Left Cheek- paired samples statistics.

Paired Samples Correlations

		N	Correlation	Sig.
Pair 3	LChAlg & LChMark	15	-.398	.142

Table 3.2. Third pair of subsets Left Cheek- paired samples correlation.

Paired Samples Test

		Paired Differences					t	df	Sig. (2-tailed)
		Mean	Std. Deviation	Std. Error Mean	95% Confidence Interval of the Difference				
					Lower	Upper			
Pair 3	LChAlg - LChMark	1.95	1.54	.39	1.10	2.81	4.909	14	.000

Table 3.3. Third pair of subsets Left Cheek- paired samples test.

The descriptive statistics of the third pair of subsets LCh (Tables 3.1-3.3), shows the mean and standard deviation of the LChAlg subset were 2.1 and 1.47 respectively, while the mean and standard deviation of the LChMark subset were lower 0.13 and 0.15 respectively, which means that the average of measuring differences was lower in the merging through markers than algorithm. LChAlg and LChMark subsets were relatively strong and negative correlated (r=-0.39, P>.001). There was a significant difference between LChAlg and LChMark subsets (t_{14}=4.9, P<.001), which means that merging by markers was significantly more accurate than merging by algorithm.

Fourth pair of subsets REr:

Paired Samples Statistics

		Mean	N	Std. Deviation	Std. Error Mean
Pair 4	RErAlg	2.00	15	1.16	.30
	RErMark	.14	15	.17	.04

Table 4.1. Fourth pair of subsets Right Ear- paired samples statistics.

Paired Samples Correlations

		N	Correlation	Sig.
Pair 4	RErAlg & RErMark	15	.085	.762

Table 4.2. Fourth pair of subsets Right Ear- paired samples correlations.

Paired Samples Test

		Paired Differences					t	df	Sig. (2-tailed)
		Mean	Std. Deviation	Std. Error Mean	95% Confidence Interval of the Difference				
					Lower	Upper			
Pair 4	RErAlg – RerMark	1.85	1.16	.30	1.21	2.50	6.176	14	.000

Table 4.3. Fourth pair of subsets Right Ear- paired samples test.

The descriptive statistics of the fourth pair of subsets REr (Tables 4.1-4.3), shows the mean and standard deviation of the RErAlg subset were 2 and 1.16 respectively, while the mean and standard deviation of the RErMark subset were lower 0.15 and 0.17 respectively, which means that the average of measuring differences was lower in the merging through markers than algorithm. RErAlg and RErMark subsets were weakly and positively correlated ($r=.085$, $P>.001$). There was a significant difference between RErAlg and RErMark subsets ($t_{14}=6.17$, $P<.001$), which means that merging by markers was significantly more accurate than merging by algorithm.

Fifth pair of subsets LEr:

Paired Samples Statistics

		Mean	N	Std. Deviation	Std. Error Mean
Pair 1	LErAlg	2.21	15	1.67	.43
	LErMark	.13	15	.15	.04

Table 5.1. Fifth pair of subsets Left Ear-paired samples statistics.

Paired Samples Correlations

	N	Correlation	Sig.
Pair 5 LErAlg & LErMark	15	-.315	.252

Table 5.2. Fifth pair of subsets Left Ear-paired samples correlation.

Paired Samples Test

	Paired Differences					t	df	Sig. (2-tailed)
	Mean	Std. Deviation	Std. Error Mean	95% Confidence Interval of the Difference				
				Lower	Upper			
Pair 5 LErAlg - LErMark	2.07	1.73	.44	1.11	3.03	4.632	14	.000

Table 5.3. Fifth pair of subsets Left Ear-paired samples test.

Tables 5.1-5.3 show the descriptive statistics of the fifth pair of subsets Left Ear, shows the mean and standard deviation of the LErAlg subset were 2.2 and 1.6 respectively, while the mean and standard deviation of the LErMark subset were lower 0.13 and 0.15 respectively, which means that the average of measuring differences was lower in the merging through markers than algorithm. LErAlg and LErMark subsets were relatively strong and negative correlated ($r=-0.315$, $P>.001$). There was a significant difference between LErAlg and LErMark subsets ($t_{14}=4.6$, $P<.001$), which means that merging by markers was significantly more accurate than merging by algorithm.

<u>Sixth pair of subsets Mental:</u>

Paired Samples Statistics

		Mean	N	Std. Deviation	Std. Error Mean
Pair 6	MenAlg	1.83	15	1.05	.27
	MenMark	.15	15	.15	.04

Table 6.1. Sixth pair of subsets Mental-paired samples statistics.

Paired Samples Correlations

		N	Correlation	Sig.
Pair 6	MenAlg & MenMark	15	-.204	.465

Table 6.2. Sixth pair of subsets Mental- paired samples correlation.

Paired Samples Test

		Paired Differences					t	df	Sig. (2-tailed)
		Mean	Std. Deviation	Std. Error Mean	95% Confidence Interval of the Difference				
					Lower	Upper			
Pair 6	MenAlg - MenMark	1.68	1.10	.28	1.07	2.29	5.927	14	.000

Table 6.3. Sixth pair of subsets Mental-paired samples test.

Tables 6.1-6.3 show the descriptive statistics of the sixth pair of subsets Mental, shows the mean and standard deviation of the MenAlg subset are 1.8 and 1.05 respectively, while the mean and standard deviation of the MenMark subset were lower 0.15 and 0.15 respectively, which means that the average of measuring differences was lower in the merging through markers than algorithm. MenAlg and MenMark subsets were relatively weak and negatively correlated (r=-0.204, P>.001). There was a significant difference between MenAlg and MenMark subsets (t_{14}=5.9, P<.001), which means that merging by markers was significantly more accurate than merging by algorithm.

The summary of the results for all six pairs subsets (Nose, RCh, LCh, REr, LEr and Ment) demonstrates that the means and the standard deviations of subsets in points group was significantly lower than those of the algorithm group.

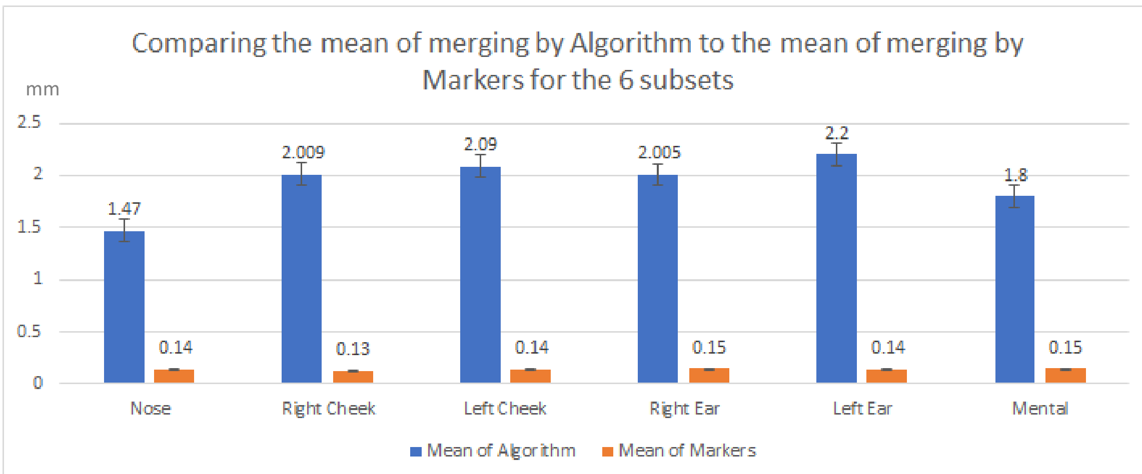

The results of this study showed that merging through markers was significantly more accurate than merging though algorithm.

CHAPTER V
DISCUSSION

The present prospective clinical study indicates the rejection of the null hypothesis and can be interpreted that merging through markers was significantly more accurate than merging through algorithm paired subsets,

The results show that mean values for the 6 subsets in the merging through algorithm were 1.47~2mm, this can cause clinically significant errors when executing a treatment plan. However, when merged by markers, the mean values were low (~0.14mm).

The results showed that the variations of the observations in the 6 subsets in the merging through algorithm varied widely, from 0.93 to-1.67mm, while the merging through markers groups exhibited almost the same variation (0.16mm) among the 6 subsets. This suggests higher confidence in creating treatment plans using markers when compared to algorithm.

The present prospective clinical study was designed to: 1) Evaluate the accuracy of using facial markers in comparison to algorithm concept in the integration of soft tissue scan with CBCT scan, 2) Propose a novel approach to integrating 3D facial scan using facial markers in 3D digital workflow, 3) Propose novel approach in integrating facial scans of patients in smile for 3D digital smile design using forehead aligner, and 4) Propose a novel integration of facial planes into a 3D digital workflow.

Previous studies[6,8,20] reported that there is difficulty in registration procedures and matching of face scans at smile because of distorted landmarks. Jivarj et al.[7] reported that the accuracy of integrated facial scanning data depends upon the visibility of maxillary anterior teeth as a fixed landmark. Hassan et al.[8] concluded that the registration accuracy of a 3D facial scan during neutral, smile, and cheek retractor using the forehead as a stable landmark is affected by facial grooving and hair, and salivary flow.[8] These drawbacks in facial scanning can be overcome, as proposed in the present study, by using fixed facial references during registration procedures with a resultant increase in matching accuracy.

Rangel et al.[6] reported that 2D images have become outmoded and of limited value in the maxillofacial region because it is now possible to represent the patient in 3D while providing information about the soft tissue profile.

The AFT System allows simple and fast 3D face scanning and presentation of the esthetic results from all view angles.[61] This software allows for design and printing of 3D virtual models and uses color data for creating an ideal smile.[59] 3D facial scan can be used to assist with fabrication of mock-ups, provisional restorations and the final definitive prostheses.[40]

Bellus3D Dental camera is a powerful and easy to use 3D face scanning app that permits the capture and integration of 3D face scans into the workflow for dentists and dental labs. Lifelike high-resolution 3D face scans are captured, displayed and automatically aligned with dental CBCT scans for interactive viewing.[60]

Stereophotogrammetry technology is one of the most common 3D surface imaging methods. It offers a number of distinct advantages: accuracy, only one scan required, archive captured images for future analysis, it is minimally invasive, and it possesses one second capture speed. This leads to accurate reproduction of facial surface geometry with realistic texture, color and resulting in a lifelike image. SPG is considered a reliable, rapid and safe method for performing facial analysis. It is a non-touch technique; hence, there is no direct contact or pressure on surfaces and consequently a high reliability of the measurements.[13,19] Dindaroglu et al.[30] reported that 3D SPG provide an accurate image of the facial soft tissues[30]

Based on the results of the current study, the paired samples descriptive statistic mean average values was lower in merging through markers than algorithm merging. These findings are in coincide with the results of Cascon et al.[58] where they reported inaccuracies in facial scanning due to small movements of the patient during capture. On the contrary, merging through markers was not affected by slight movement due to the stability of the fixed points during merging processes.

There was statistically significant difference between merging through markers and merging by algorithm. The results of the present study validate the previous findings of Cascon et al.[58] where it was found that a significant difference existed between manual and digital inter-landmark measurements using a dual-structured light facial scanner. Plooij et al.[13] reported that there was a discrepancy in the mean value between digital and manual inter-landmark measurements (0.91 ±0.32 mm) which was clinically acceptable during digital steps for treatment planning of the virtual face.

The results of the current study are in contrast with the findings of Hassan et al.[8] and Rangel et al.[6] where they concluded that digital integration of facial scanning for edentulous patient is inaccurate tool. They attributed the inaccuracy in registration and matching procedures to using forehead as a landmark that altered the facial anatomy.

In the present study the paired samples test showed a significant differences ($P<.001$) between merging through markers and merging by algorithm. The accurate merging through markers, rather than by algorithm, could be attributed to using the same fixed facial reference radiopaque markers during registration procedures.

The results of this study are in contrast with the findings of Maal et al.[57] it was found that a relatively large registration error at lateral neck and around mouth, and the eyes between the textured and untextured skin surfaces. This error was caused by various facial expressions and head positioning during image acquisition. Swennen et al.[42] using CT instead of CBCT and reported a large registration error around cheeks due to gravity while the patient in supine position, however, in the current study by using CBCT with the patient seated in upright position. Naudi[44] stated that the upright position during CBCT scan preserving the soft tissue shape.

A limitation of this study is the observation of a high standard deviation compared with means, which might be correlated with a low sample size or the size of the RO marker used in measurements. Further studies should be made to assess the accuracy of merging dental casts (3D model) with a facial scan and their application to use on a virtual articulator in a 3D digital workflow.

CHAPTER VI

CONCLUSIONS

Within the limitations of this study, the following conclusions may be drawn:

1. 3D facial scan merging to CBCT using RO radiographic markers was significantly more accurate than alterative closest point algorithm.
2. 3D Facial scan can be used with markers as an alternative to 2D pictures in digital treatment planning and digital waxing.
3. Merging CBCT dataset with facial scan can reliably visualize patients hard and soft tissues. This may allow for improved accuracy during digital smile design, implant planning and may improve treatment outcomes.

CHAPTER VII

BABILLOGRAPHY

1. Rufenach CR. Fundamentals of esthetics. Chicago: Quintessence; 1990.   p.121–7.

2. Mclaren EA, Schoenbaum T. Digital photography enhances diagnostics, communication, and documentation. Compend Contin Educ Dent 2011;32:36–8.

3. Lin WS, Harris BT, Phasuk K, Llop DR, Morton D. Integrating a facial scan, virtual smile design, and 3D virtual patient for treatment with CAD-CAM ceramic veneers: a clinical report. J Prosthet Dent 2018;119:200–5.

4. Goodacre CJ, Garbacea A, Naylor WP, Daher T, Marchack CB, Lowry J. CAD/CAM fabricated complete dentures: concepts and clinical methods of obtaining required morphological data. J Prosthet Dent 2012;107: 34–46.

5. Spear FM, Kokich VG. A multidisciplinary approach to esthetic dentistry. Dent Clin North Am 2007;51:487–505.

6. Rangel FA, Maal TJ, Bergé SJ, van Vlijmen OJ, Plooij JM, Schutyser F, et al. Integration of digital dental casts in 3-dimensional facial photographs. Am J Orthod Dentofacial Orthop 2008;134:820–6.

7. Jivraj S, Chee W, Corrado P. Treatment planning of the edentulous maxilla. Br Dent J 2006;201:261–79.

8. Hassan B, Greven M, Wismeijer D. Integrating 3D facial scanning in a digital workflow to CAD-CAM design and fabricate complete dentures for immediate total mouth rehabilitation. J Adv Prosthodont 2017;9:381–6.

9. Bowen AA, Javier AF, Rodríguez.NA. Digital work flow in implantology using facial scanner. Ciencia 2018;300:216–32.

10. Ji Y, Zhang F, Schwartz J, Stile F, Lineaweaver WC. Assessment of facial tissue expansion with three-dimensional digitizer scanning. Craniofac Surg 2002;13:687–92.

11. Aldridge K, Boyadjiev SA, Capone GT. Precision and error of three-dimensional phenotypic measures acquired from 3DMD photogrammetric images, Am.J.Med. Genet 2005;13:243–47.

12. Weinberg SM, Kolar JC. Three-dimensional surface imaging: limitations and considerations from the anthropometric perspective. J Craniofac Surg 2005;16:847–51.

13. Plooji J, Maal T. Digital three-dimensional image fusion processes for planning and evaluating orthodontics and orthognathic surgery: a systematic review. Int J Oral Maxillofac Surg 2011;40:341–52.

14. Shaner DJ, Bamforth JS, Peterson AE, Technical note: different techniques, different results--a comparison of photogrammetric and calliper-derived measurements, Am J Med Phys Anthropol1998;106:547–52.

15. Ma l, Xu T, Lin J. Validation of a three-dimensional facial scanning system based on structured light techniques. In Computer methods and programs in biomedicine 2009;94:290–8.

16. Marmulla R, Hassfeld S, Ligh T, Muhling J. Laser-scan-based navigation in cranio-maxillofacial surgery. J Craniomaxillofacial Surg 2003;31:267–77.

17. Moss JP, Ismail SF, Hennessy RJ. Three-dimensional assessment of treatment outcomes on the face. Orthod Craniofac Res 2003; 6:126–31.

18. Kau CH, Richmond S, Alexei I. Zhurov AI, AL Knox J, Chestnutt I, Hartles F, et al. Reliability of measuring facial morphology with a 3-dimensional laser scanning system. Am J Orthod Dentofacial Orthop 2005;128:424–30.

19. Heike CL, Upson K, Stuhaug E, Weinberg SM. 3D digital stereophotogrammetry: a practical guide to facial image acquisition. Head Face Med 2010;6:18–26.

20. Joda T. Brägger U, Gallucci G. Systematic literature review of digital three-dimensional superimposition techniques to create virtual dental patients. Int J Oral Maxillofac Implants 2015;30:330–7.

21. Leung MY, Lo J, Leung YY. Accuracy of different modalities to record natural head position in 3 dimensions: a systematic review. J Oral Maxillofac Surg 2016;74:261–84.

22. Hassan B, Gonzalez GB, Tahmaseb A, Jacobs R, Bornstein MM. Three-dimensional facial scanning technology: applications and future trends. Forum Implantologicum 2014;10:78–86.

23. Farkas LG, Posnick JC, Horeczko TM. Anthropometric growth study of the head. Cleft Palate Craniofac J 1992;29:303–8.

24. Dimaggio FR, Ciusa V, Sforza C, Ferrario VF. Photographic soft-tissue profile analysis in children at 6 years of age. Am J Orthod Dentofacial Orthop 2007; 132:475–80.

25. Bavbek NC, Tuncer BB, Tortop T. Soft tissue alterations following protraction approaches with and without rapid maxillary expansion. J Clin Pediatr Dent 2014;38:277–83.

26. Baik H-S, Kim S-Y. Facial soft-tissue changes in skeletal Class III orthognathic surgery patients analyzed with 3-dimensional laser scanning. Am J Orthod Dentofacial Orthop 2010;138:167–78.

27. Palomo JM, Chrestopher M, Hans M.The accuracy and reliability of CBCT measurement. Int J oral Maxillofac Surg 2007;21:S422–S6.

28. Cutting CB, McCarthy JG, Karron DB. Three-dimensional input of body surface data using a laser light scanner. Ann Plast Surg 1988;21:38–45.

29. kochel J, Meyer-Marcotty P, Stmad F, Kochel M, Stelzig-Eisenhauer A. 3D soft tissue analysis- Part1: sagittal parameters. J orofac Othop 2010;71:40–52.

30. Dindaroğlu F, Kutlu P, Duran GS, Görgülü S, Aslan E. Accuracy and reliability of 3D stereophotogrammetry: A comparison to direct anthropometry and 2D photogrammetry. The Angle Orthod 2016;86:487–94.

31. Tapie L, Lebon N, Mawussi B, Fron Chabouis H, Duret F, Attal JP. Understanding dental CAD/CAM for restorations - the digital workflow from a mechanical engineering viewpoint. Int J Comput Dent 2015;18:21–44.

32. Joo HS, Park SW, Yun KD, Lim HP. Complete-mouth rehabilitation using a 3D printing technique and the CAD/CAM double scanning method: A clinical report. J Prosthetic Dent 2016;116:3–7.

33. Monaco C, Ragazzini N, Scheda L, Eangelisti E. A fully digital approach to replicate functional and aesthetic parameters in implant – supported full arch rehabilitation. J Prosthodontic Res 2018;62:383–5.

34. Mclaren EA. Bonded functional aesthetic prototype an alternative pre-treatment mock-up technique and cost effective medium-term esthetic solution. Compend Contin Edu Dent 2013;34:596–607.

35. Monaco CT, Arena A, Palotti G, Scheda L. Digital bar prototype technique for full-arch rehabilitation on implants. JADA 2019;150:549–55

36. Gabriele C, Luca F, and Alina V. Dental Restorative Digital Workflow: Digital Smile Design from Aesthetic to Function Dentistry Journal 2019;7:1–12.

37. Mclaren EA, Chang YY .photography and Photoshop, simple tool and rules for effective and accurate communication. Inside Dentistry 2006;2:97–101.

38. Zimmermann M, Mehl A. Virtual smile design systems: a current review. Int J Comput Dent 2015;18:303–17.

39. Coachman C, Calamita MA. Digital smile design: A tool for treatment planning and communication in esthetic dentistry. Quintessence Dent Technol 2012;35:103–11.

40. Coachman C, Calamita MA, Sesma N. Dynamic Documentation of the Smile and the 2D/3D Digital Smile Design Process The International Journal of Periodontics & Restorative Dentistry 2017;37:183–92.

41. Holberg C, Schwenzer K, Rudzki-Janson I. Three-dimensional soft tissue prediction using finite elements. Part I: Implementation of a new procedure. J Orofac Orthop 2005:66:110–21.

42. Swennen GR, Schutyser F, Barth EL, De Groeve P, De Mey A. A new method of 3-D cephalometry. Part I: the anatomic Cartesian 3-D reference system Craniofac Surg 2006:17:314–25.

43. Moro A, Correra P, Boniello R, Gasparini G, Pelo S. Three-dimensional analysis in facial asymmetry: comparison with model analysis and conventional two-dimensional analysis. J Craniofac Surg 2009;20:417–22.

44. Naudi K B, Benramadan R, Brocklebank L, Ju X, Khambay B, Ayoub A. The Virtual Human Face: Superimposing the Simultaneously Captured 3D Photorealistic Skin Surface of the Face on the Untextured Skin Image of the CBCT Scan. Int J Oral Maxillofac Surg 2013;42:393–400.

45. Eaton KA, Raynolds PA, Grayden SK, Wilson NH, Jones M L, Pine C, Saunders WP. A vision of dental education in the third millennium .Br Dent J 2008;205:261–71.

46. Fasbinder DJ. Digital dentistry: innovation for restorative treatment. Compend Contin Educ Dent 2010;31:2-11.

47. Glossary of digital dental terms. J Prosthodont 2016;25:S2–S9.

48. Gimenez-Gonzalez B, Hassan B, Ozcan M, Pradies G. an in vivo study of factors influencing the performance of digital intraoral impressions Operating an active wavefront sampling technology with multiple implants in the edentulous maxilla.: J Prosthet Dent. 2017;26:650–5.

49. Hassan B, Gimenez Gonzalez B, Tahmaseb A, Greven M, Wismeijer D. A digital approach integrating facial scanning in CAD/CAM workflow for full mouth implants supported rehabilitation of the edentulous patient: A pilot clinical study. J Prosthet Dent 2016;117:486–92. In Press

50. Leon MR, Torre AB, Rubio JL, Faberga JJ, Ozcan M. Digital tool and 3D printing technologies integrated into the workflow of restorative treatment: A clinical report. Journal of Prosthetic Dentistry 2019;121;3–8.

51. Neal P. Integrating three-dimensional digital technologies for comprehensive implant dentistry. J Am dent Assoc 2010;141:20S–4S.

52. EXOCAD: Align Technology to Acquire Global Dental CAD/CAM Software Leader Exocad, Global Newswire.

53. Scarfe WC, Farman AG, Sukovic P. Clinical applications of cone-beam computed tomography in dental practice. J Can Dent Assoc 2006;72:75–80.

54. Sahithya K. CBCT -Cone Beam Computed Tomography. Journal of Academy of Dental Education 2014;1:9–15.

55. Venkatesh E, Elluru SV. Cone beam computed tomography: basics and applications in dentistry. J Istanb Univ Fac Dent 2017;51:S102– S21.

56. Lee CY, Ganz SD, Wong N, Suzuki JB. Use of cone beam computed tomography and a laser intraoral scanner in virtual dental implant surgery part 1 Implant Dent 2012;21:265–71.

57. Maal TJ, Plooij JM, Rangel FA, Mollemans WF, Schutyser AC. Berge SJ. The accuracy of matching three-dimensional photographs with skin surfaces derived from cone-beam computed tomography. Int. J. Oral Maxillofac. Surg 2008;37:641–6.

58. Cascon WP, De Gopegui JR, Revilla M. Facially generated and additively manufactured baseplate and occlusion rim for treatment planning a complete-arch rehabilitation: A dental technique. J Prosthet Dent 2019;121:741–5.

59. Daher R, Ardu S, Vjero O, Krejci I. 3D Digital Smile Design with a Mobile Phone and Intraoral Optical Scanner. Compend Contin Educ Dent 2018;39:e5–e8.

60. Bellus3D: High-quality 3D face scanning, Bellus3D user manual.

61. AFT Dental system, AFT System One user manual.